CHEMICAL ENGINEERING TRANSACTIONS
VOL. 65, 2018

A publication of
AIDIC
The Italian Association of Chemical Engineering
Online at www.aidic.it/cet

Guest Editors: Eliseo Ranzi, Mario Costa

ISBN 978-88-95608- 62-4; **ISSN** 2283-9216

Benefit of Fe-containing catalytic systems for dry reforming of lignin to syngas under microwave radiation

M.D.Tsodikov[a], O.G.Ellert[b], O.V.Arapova[a], S.A. Nikolaev[c], A.V.Chistyakov[a], Yu.V.Maksimov[d]

[a]Topchiev Institute of Petrochemical Synthesis RAS, Leninskii pr. 29, Moscow 119991, Russia
[b] Kurnakov Institute og General and Inorganic Chemistry Leninskii pr. 31, Moscow 119991, Russia
[c] M. V. Lomonosov Moscow State University, Moscow, Russia
[d] Semenov Institute of Chemical Physics RAS, Kosygina str., 4, Moscow 119991, Russia
arapova@ips.ac.ru

Fe-containing nanoparticles provide for high-rate microwave-assisted dehydrogenation and dry reforming of lignin into syngas without additional carbon sorbent. Lignin samples were obtained by deposition of iron from the acetylacetonate complex and contained 0.05; 0.10; 0.50; 1.50; and 2.0 wt.% Fe, respectively. According to another procedure, iron particles were deposited from a colloid solution of metal particles in toluene prepared by metal vapor synthesis. The obtained sample contained 2.8 wt.% Fe. Study of the microwave-assisted heating dynamics for a number of solid lignin samples with different Fe concentrations revealed the threshold concentration, 0.5 wt % Fe, which ensures the highest heating rate up to the temperature of reforming and plasma ignition. Increasing of Fe content up to 2% led to an increasing selectivity towards syngas production. The process of reforming proposed in this work provides a 90-94 % recovery of hydrogen from lignin. These results suggest that the conversion of lignin follows two pathways giving hydrogen and syngas accompanied by compaction of fused polyaromatic structures to graphitized carbon, which is formed in 35-40% yield.

1. Introduction

The processes of dry reforming of methane and other hydrocarbons are usually accompanied by the deposition of carbon, which can lead to catalyst poisoning. This is the main reason, which makes the development of the industrial processes complicated. Lignin reforming process is free of this disadvantage and is used for solid waste disposal and for providing important energy carries. Importantly, in this process greenhouse gases are utilized. It is also well known that syngas is raw feedstock for producing methanol, diethyl ether and fuel components. It should be mentioned that the processes of synthesis on the base of CO and H_2 are exothermic. Thus the heat released during these processes can compensate the energy expenses of the endothermic dry reforming process. It is known that some organic substrates are capable of absorbing microwave radiation (MWR). This ability ensures fast heating up to plasma generation and results in efficient pyrolysis of raw feedstock (Yunpu, 2016). In recent years, MWR has been used for the catalytic cracking of lignin in the presence of heterogeneous catalysts (Antonetti, 2017; Zhang, 2003). However, the dielectric losses of lignin determining the level of MWR absorption are too low to attain the temperature of cracking and pyrolysis. Therefore, effective MWR sorbents possessing a high dielectric loss tangent like carbon, metal nanoparticles, and Fe, Co, and Ni carbides are added to lignin. High density of dispersed metals or alloys, their weak magnetocrystalline anisotropy and low permeability can limit their applicability at high frequencies (Rousselle, 1993). It is possible to create effective catalysts simultaneously working as MWR absorbers in MWR assisted dry reforming of lignin. The main idea is that after impregnation with a solution containing Fe ions nanoparticles of a few nanometers in size are formed on the lignin surface. Some of them can have core-shell type of structure. Under subsequent MWR impact these particles begin to work as effective MWR sorbents and catalysts. It was earlier reported that Fe containing core-shell nanoparticles efficiently absorb

MWR (Lu, 2008). We assumed that Fe nanoparticles formed on lignin surface as a result of impregnation efficiently interact with surface functional groups that facilitate the formation of particle core-shell microstructure. During heating under MWR and subsequent plasma ignition Fe-containing nanoparticles encapsulated in carbon can be formed. Such type of the particles can promote substrate heating up to the temperature of reforming within shortest possible time without additional MWR sorbents. In the present work we report on heating dynamics of lignin samples with different concentrations of Fe containing MWR absorbing agents and lignin conversion results. Microstructure and magnetic properties of the samples before and after MWR dry reforming are also considered.

2. Materials and Methods

Lignin (mixed, wood origin, Kirov Region, Russian Federation). Composition, wt. %: C - 58.1; H - 5.4; Al - 1.2; Si - 3.1; Ca - 0.6; Fe - 0.8; Mg - 0.04; S - 1.2; N - 0.2; O - 28.9, other elements - 0.5 (less than 0.05% of each element). Reagents, solvents, and gases: toluene (Sigma-Aldrich) and $Fe(acac)_3$ (Aldrich). Iron acetylacetonate $Fe(acac)_3$ (Aldrich) was used for deposition on the lignin surface.

Lignin mixtures with an iron catalyst were prepared by two different procedures, both aimed at the formation of nano-sized iron particles on the lignin surface. According to the first procedure, iron was deposited from ethanol solutions of iron acetylacetonate with various concentrations via impregnation of lignin with a moisture capacity of 4 cm^3/g. Solutions containing 0.08, 0.17, 0.83, 2.46, or 3.25 wt. % of iron acetylacetonate were slowly added to 4 g of lignin with shaking. Then the lignin sample was kept for two hours in a closed vessel with stirring at intervals. The wet lignin was dried in air at room temperature for 24 hours and in a drying oven at 110 °C for 2 hours. The iron content on the lignin surface was determined by atomic absorption spectrometry. Thus, lignin samples were obtained by deposition of iron from the acetylacetonate complex; samples 1–6 contained 0.05; 0.10; 0.50; 1.50; and 2.0 wt.% Fe, respectively. Samples 5 and 6 contained equal percentages of iron (2.0%) and were used in experiments carried out in Ar and CO_2 atmospheres (Table 1). According to the second procedure, iron particles were deposited from a colloid solution of metal particles in toluene prepared by metal vapor synthesis (MVS) (Rubina, 2016). This procedure was used to obtain sample 7 containing 2.8 wt.% Fe. After deposition, the sample was dried in air for 10 h and then in a vacuum oven at a temperature of 60-80 °C and a residual pressure of 1 Torr.

The process flowchart and the unit for lignin conversion have been described in detail (Arapova, 2017a). The dry reforming was carried out in a 15 cm^3 flow type quartz reactor. The reactor was mounted in the wave guide of a microwave setup equipped with a 540W magnetron M-140 generating a microwave radiation at a 2.45 ± 0.05 GHz frequency and 100–150 mA current densities. The temperature in the reactor was determined by a previously described procedure using a tungsten rhenium thermocouple placed into a reactor well. The carbon dioxide reforming was carried out according procedure reported earlier (Tsodikov, 2017). Carbon dioxide was fed to the reactor bottom at a 60 cm^3/min flow rate and induced temperature of 750-800 °C. For comparison, experiments on microwave irradiation of iron-containing lignin under Ar were carried out. Experiments on reforming induced by convective heating at 750-800 °C and CO_2 flow rate of 60 cm^3/min were carried out for comparison with the results of microwave-assisted lignin conversion. Gaseous reaction products were analyzed online by gas chromatography on a Kristallux-4000 M chromatograph. The hydrocarbon fraction was analyzed using a 1.5 m packed column filled with a-Al2O3 grains (0.5 mm) with 15% of supported squalane phase using a flame ionization detector (FID) and He as the eluent. The contents of H2, CH4, CO and CO2 were determined using thermal conductivity detector (TCD) and Ar as the eluent The conversion of lignin (α,%) was defined as: $m_l \times C(\%) - m_{res.} \times C(\%) / m_l \times C(\%)$, where m_l – mass of lignin, m_{res} – mass of residue. X-ray diffraction, transmission electron microscopy and magnetic properties of iron-containing samples were carried out according procedure reported earlier (Tsodikov, 2017). The ^{57}Fe Mössbauer spectra were recorded on a Wissel electrodynamic type spectrometer (Germany) at 300 K using a Janis (CCS-850) helium cryostat with a Lake Shore Cryotronics (332) temperature controller. The accuracy of temperature maintenance was at least 0.1 K. As the radiation source, 57Co(Rh) with 1.1 GBq activity was used. The isomer shifts were referred to the center of the iron metal magnetic hyperfine structure. The Mössbauer spectra were treated using least squares calculation software (LOREN, Institute of Chemical Physics RAS; WINNORMOS, Germany) assuming the Lorentzian line shape. For enhanced sensitivity of Mössbauer spectroscopy, ^{57}Fe-enriched acetylacetonate and acetylacetate were used, which were synthesized by a reported procedure (Ellert, 1996).

3. Results and Discussion

The heating dynamics observed upon MWR of the initial lignin and Fe-containing samples of different Fe concentration is presented in Fig.1. The samples bearing supported iron particles demonstrate a pronounced ability to absorb MWR and are heated rather rapidly, with plasma being generated on the surface (Fig.1). The deposition of only 0.05% Fe (sample 1, Table 1) results in considerable acceleration of heating compared to the initial lignin containing 0.8% of natural iron. At that the reforming temperature (750-800° C) is attained in approximately 40 s after an induction period of 60 s. The increase in the iron concentration up to 0.5 wt.% Fe (sample 3, Table 1) results in a stepwise temperature rise and plasma generation. Attention is attracted by the qualitative change in the heating curves for samples with iron concentrations higher than the threshold value 0.5 wt.% Fe. These samples give rise to gently sloping heating curves without an induction period. The complex heating dynamics of Fe-containing lignin samples points to that the capacity for MWR absorption is determined by not only Fe concentration but also by the nature of the metal, particle size and microstructure. This is confirmed, for example, by the fact that unlike Ni-containing lignin samples prepared by the same procedure (Tsodikov, 2017), the impregnation of lignin with the solution containing Fe ions results in the high microwave absorption and fast substrate heating up to the reforming temperature without additional carbon sorbent and plasma ignition on the surface.

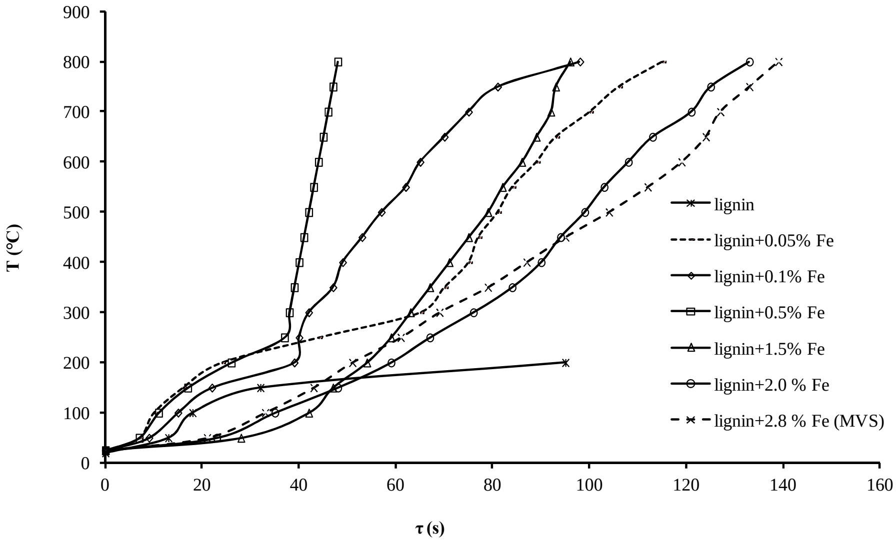

Fig. 1. Heating dynamics of the initial lignin and Fe-containing samples.

The MWR-induced carbon dioxide reforming of Fe-containing samples gives mainly gaseous products containing H_2, CO, CH_4, and a slight amount of C_2-C_4 hydrocarbons (Table 1).

Table 1. Lignin conversion products and selectivity to synthesis gas

N/N	Fe, wt.%	Oil, wt.%	Char, wt.%	Gas, wt.%	Gas composition, mol.%				S_{H_2+CO}, %
					H_2	CO	CH_4	C_2-C_4	
				Microwave heating					
1	0.05	4.9	42.5	52.6	31.2	50.1	14.8	3.9	81.3
2	0.1	3.5	42.2	54.2	35.4	45.6	15.3	3.8	80.9
3	0.5	7.4	43.3	49.3	42.8	41.1	13.4	2.8	83.9
4	1.5	1.8	43.7	54.5	38.9	50.0	9.5	1.6	89.0
5*	2.0	3.3	47.9	48.8	52.4	37.7	8.9	1.0	90.1
6	2.0	1.0	40.2	58.8	43.8	49.6	5.8	0.0	94.1
7	2.8 (MVS)	0.3	41.3	58.4	42.8	48.7	7.5	1.1	91.4
				Convective heating					
8	0	38.9	41.8	19.3	12.3	56.4	28.4	3.0	24.2
9	1.5	22.2	51.5	26.3	25.6	39.9	32.2	2.3	34.5

* *The conversion of lignin was performed in an Ar flow*

An increase in the Fe content from 0.5 to 2.0% markedly increases the selectivity to synthesis gas from 75 to 94%, with the H_2/CO ratio being ~ 0.9. At low iron density on the surface under MWI a part of organic mass of lignin most likely undergoes thermolysis resulting in the increase of methane yield.

The degree of conversion of Fe-containing lignin being equal to α ~55-60% virtually does not depend on whether the reforming is carried out in Ar or CO_2 atmosphere. Correspondingly, the amount of the carbon residue is also approximately the same and does not depend on the concentration of the Fe-containing catalyst (Table 1). These results differ from those obtained for Ni-containing lignin for which the lignin conversion under MWR in the presence of a carbon adsorbent is higher by 10% in CO_2 than in Ar atmosphere (Tsodikov, 2017). The Fe-containing lignin samples display 90% selectivity in Ar flow and the H_2 content in the syngas markedly increases while the CO content decreases (Table 1, sample 5), whereas in CO_2, the H_2/CO ratio in the syngas is 0.9. According to our results the ratio H_2/CO in Ar flow is higher than in CO_2 (Table 1, 5^* and 6). This result possibly is due to the dehydrogenation reaction development. Recently we showed that under MWI and plasma regime the destruction of C-H terminal bonds occurs in organic compounds (Tsodikov, 2016). The reforming of the initial lignin under convective heating gives rise to the formation of water-cut liquid aromatic compounds. According to the IR spectroscopy data, the aromatic compounds were represented by vaniline derivatives, guaiacols, and alkyl-substituted phenols (Arapova, 2017b). With the convective heating of iron-containing sample (Table 1, sample 9), the conversion decreases by only 10%. The selectivity to syngas markedly declines in this case, because aromatic hydrocarbons and water predominate in the reaction products. It is also noteworthy that increasing the Fe content on the lignin surface up to 2.0 wt % under MWR leads to a considerable increase in the content of syngas and decrease in the content of C_2-C_4 hydrocarbons and mainly methane (Table 1). The results provide the conclusion that microwave-assisted reforming on iron sites involves the transformation of terminal methoxy groups and lignin destruction products that have been identified for convective heating (guaiacols, and aniline derivatives) to give gaseous products among which synthesis gas predominates. The catalytic contribution of Fe-containing systems to lignin transformation is manifested as increasing selectivity to syngas.

X-Ray diffraction data showed that the phase compositions of initial lignin and iron-modified lignin before and after catalysis are quite similar. Along with the substantial amount of organic phase the samples contain SiO_2 and aluminum silicate phase $K_{0.93}Fe_{0.27}Al_{0.75}Si_{3.01}O_8$. After reforming the reflections assigned to ferric carbide compounds and carbon appear. The detailed examination made it possible identifying certain crystallographic planes for γ-Fe stabilized by carbon, $C_{0.12}Fe_{1.88}$ and $C_{0.09}Fe_{1.91}$. The reflections which can be referred to Fe_3O_4, hexagonal graphite and orthorhombic carbon have been also observed.

Transmission electron microscopy (TEM) and Mössbauer spectroscopy examination as well as magnetic measurements have been carried out before and after reforming for samples 3, 6, and 7 (Table 1) with supported iron concentrations of 0.5, 2.0, and 2.8 wt. %, respectively.

According to the TEM data samples 3 and 6 obtained by impregnation of lignin with $Fe(acac)_3$ solution contain Fe- nanoparticles. The size of these particles varies in the range from 1 up to 4 nm, besides more than 80 % of them are as large as 1±0.3 nm. Unlike single particles observed on the surface of samples 3 and 6, most particles of sample 7 obtained by impregnation with Fe-containing organosol, appeared to be in close contact with one another and form extended chains and agglomerates. The average size of detectable particles in this sample is 3 nm. During the reaction, the microstructure of samples 3, 6 and 7 undergoes considerable changes. MWR-assisted heating of the reaction mixture causes particle agglomeration approximately from 1 up to 6 nm. Interestingly, that about 45% Fe-containing nanoparticles in sample 3 (0.5 wt.% Fe) and 30% in sample 6 (2.0% wt.% Fe) are of core-shell structure. The Fe/C intensity ratio for the EDA spectra of particle edge and center shows that the core mainly consists of iron, whereas the shell is highly enriched in carbon. HRTEM image of the core-shell particle on the lignin surface after reforming of sample 6 is presented in Fig. 2. The formation of core(Fe)-shell(C) particles is apparently due to lignin destruction under MWR and plasma conditions on Fe particles followed by enveloping of the particle surface by carbon-containing fragments. The calculation of interplanar spacing *d* for the shell of such a particle yields *d* =3.6 Å, which coincides with *d* for the C(002) face. The faces with *d* = 1.47, 2.43, 3.6, and 4.2 Å are also present on the particle surface. Considering the measurement error (±0.3 Å) and the possibility of dissolution of some carbon in Fe-containing oxide, the interplanar spacings of 4.2, 2.43, and 1.47 Å can be assigned to Fe_3O_4 identified by X-ray diffraction as well.

The Mössbauer spectroscopy and magnetic measurements shed light on the complex electronic structure and cooperative spin interactions in the system of Fe-containing nanoparticles before and after reforming. These results also can help to reveal the main difference between two synthetic approaches of the Fe-containing nanoparticles formation on the lignin surface, namely: impregnation from $Fe(acac)_3$ solution and from organosol preliminary obtained by MVS. The most significant distinctive feature of the Mössbauer spectrum recorded after microwave radiation is the presence of a single line with the isomer shift δ = –0.08

mm/s, which characterize small γ-Fe clusters or, more precisely, γ-Fe-C_n clusters (David, 2011; Yamada, 2010; Yao, 2004). Under MWR, a considerable fraction of small, ~1-3 nm, superparamagnetic clusters are agglomerated forming larger superparamagnetic clusters of non-stoichiometric magnetite with a relative content of ~30-35%.

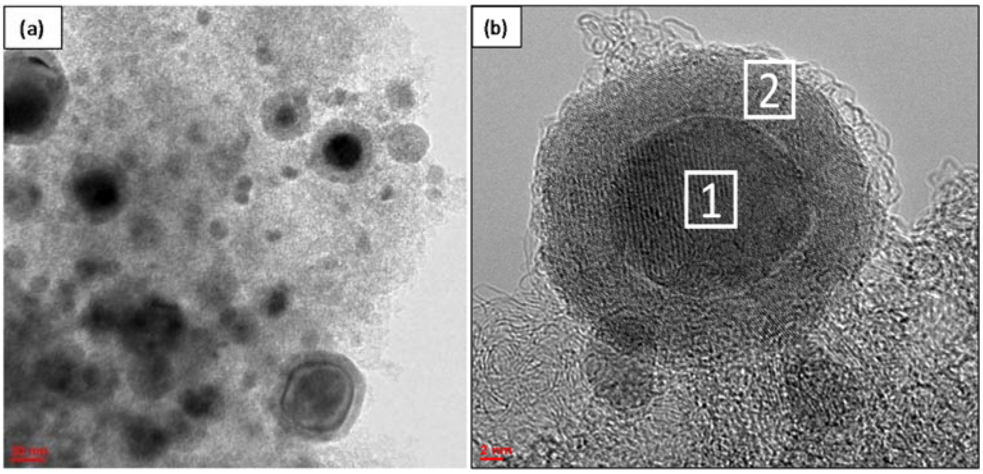

Fig. 2. (a) and (b) Micrographs of active components after the reaction.

The area of the γ-Fe-C_n single line is ~ 20% of the area of the whole spectrum. Since sample 6 contains ~ 30% of core-shell particles according to TEM examination, it can be roughly estimated that the iron-carbon compounds are formed exactly in these particles. The reflections for the iron-carbon compounds and Fe_3O_4 are also detected in the X-ray diffraction patterns.

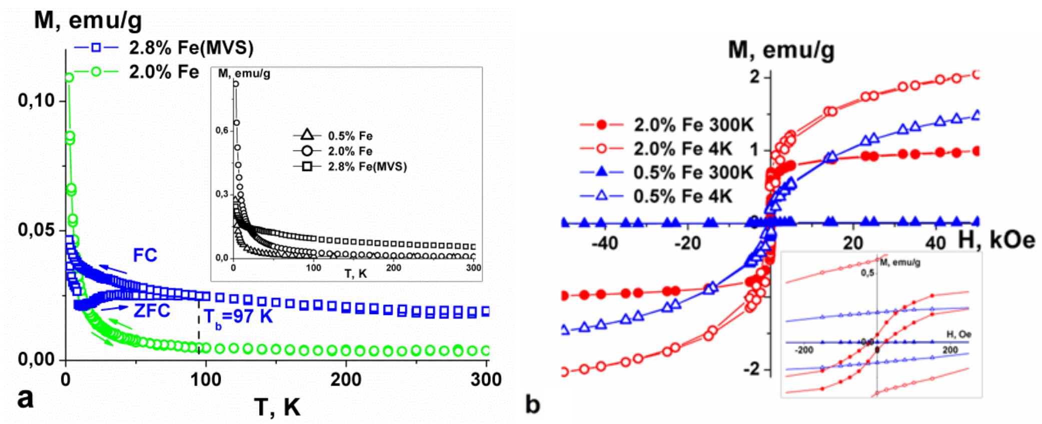

Fig.3 (a) Temperature dependence of the magnetization (M) in a H = 500 Oe field for initial (before the reforming) samples 6 (○) and 7 (□) recorded in the FC and ZFC modes. The inset shows the M(T) curves for samples 3, 6, and 7 measured in a H = 5 kOe field; (b) M(H) curves for samples 3 and 6 at T = 300 and 4 K after the reforming. The inset shows the hysteresis loops for low fields at T = 300 and 4 K (residual Mr=0.6 emu/g and Mr=0.06 emu/g for 4 and 300 K, respectively; saturation Ms=1.51 emu/g and Ms=0.84 emu/g for 4 and 300 K, respectively).

The magnetic measurements in H = 5 kOe did not reveal any difference in magnetic behavior of the samples obtained by impregnation from $Fe(acac)_3$ solution (samples 3 and 6) and from organosol sample 7 (Insert, Fig. 3a). The careful magnetic characterization of these samples showed tha they are overall paramagnetic. Meanwhile the measurements in low magnetic field, H = 500 Oe, showed that unlike sample 6, the FC and ZFC curves for sample 7 diverge at T = 97 K and at T = 8 K a magnetic phase transition occurs (Fig. 3a). We argue that magnetic properties of sample 7 are characteristic for the superpamagnetic system of Fe-containing particles. It should be mentioned that Ni –containing nanoparticles deposed on lignin surface from organosol (Tsodikov, 2017) and Fe –containing particles demonstrate similar magnetic behavior. The magnetic characterization including the dependence of magnetization, M, on the magnetic field for the samples 3 and 6 after reforming (Fig. 3b) confirms X-ray, TEM and Mössbauer spectra data, pointing to that the phase composition of deposited active components consists of about 60% of Fe_3O_4 nanoparticles and also of ~40% of the core (Fe_3O_4)@shell (nonstochiometric γ-Fe-C_n) nanostructures.

4. Conclusion

High-rate dehydrogenation and dry reforming of lignin to syngas has been carried out in the presence of Fe-containing catalytic systems under microwave radiation. Active Fe-containing nanoparticles have been preliminary formed on the lignin surface according to different synthetic approaches, namely the deposition from an ethanol solution of Fe(acac)$_3$ and from a colloid solution of iron metal particles. These nanoparticles are able to absorb microwave radiation and are suitable for microwave-assisted dry reforming with the CO/H_2 ratio of ~0.9. The catalytic performance of iron-based nanoparticles towards the lignin conversion is manifested as increasing selectivity to hydrogen and syngas, which reaches 94% at the Fe concentration of 2 wt.%. TEM, Mössbauer spectroscopy and magnetic measurements revealed the difference in microstructure and properties of obtained nanoparticles.

Acknowledgments

This work was supported by the Russian Foundation for Basic Research of Project No. 16-29-106-63.
The magnetic measurements were carried out within the State Assignment of Fundamental Research to the Kurnakov Institute of General and Inorganic Chemistry using the equipment of the JRC PMR IGIC RAS.

References

Antonetti C., Melloni M., Licursi D., Fulignati S., Ribechini E., Rivas S., Parajó J.C., Cavani F., Raspolli Galletti A.M., 2017, Microwave-assisted dehydration of fructose and inulin to HMF catalyzed by niobium and zirconium phosphate catalysts, Appl. Catal. B. Env. 206, 364-377.
Arapova O.V., Tsodikov M.V., Chistyakov A.V., Konstantinov G.I., 2017a, Dry Reforming of Kraft Lignin under MWI Action, Chemical Engineering Transactions, 57, 223-228.
Arapova O.V., Bondarenko G.N., Chistyakov A.V., Tsodikov M.V., 2017b, Vibrational Spectroscopy Studies of Structural Changes in Lignin under Microwave Irradiation, Russ. J. Phys. Chem. A, 91 (9), 1717–1729.
David B., Pizúrová N., Schneeweiss O., Kudrle V., Jašek O., Synek P., 2011, Iron-Based Nanopowders Containing α-Fe, Fe_3C, and γ-Fe Particles Synthesised in Microwave Torch Plasma and Investigated with Mössbauer Spectroscopy, Japan. J. Appl. Phys, 50.
Ellert O.G., Petrunenko I.A., Tsodikov M.V., Bukhtenko O.V., Kochubey D.I., Maksimov Yu.V., Dominguez-Rodriguez A., 1996, Study of the formation mechanism of complex oxides obtained by the sol-gel method: influence of the structure of iron, aluminium and yttrium acetylacetonate precursors on the phase composition of the ZrO_2 ceramics, J. Mater. Chem., 6, 207-212.
Lu B., Dong X.L., Huang H., Zhang X.F., Zhu X.G., Lei J.P., Sun J.P., 2008, Microwave absorbtion properties of core/shell-type iron and nickel nanoparticles, J. Magn. Magn. Mater., 320, 1106-1111.
Rousselle D., Berthault A., Acher O., Bouchaud J.P., Zerah P.G., 1993, Effective medium at finite frequency: Theory and experiment, J. Appl. Phys., 74, 475-479.
Rubina M.S., Kamitov A.A., Zubavichus Ya.V., Naumkin A.V., Suzer S.S., Vasil'kov A.Yu., 2016, Collagen-Chitosan Scaffold modifying with Au and Ag nanopatrticles: synthesis, structure and properties, Appl. Surf. Sci., 366, 365-371.
Tsodikov M.V., Konstantinov G.I., Chistyakov A.V., Arapova O.V., Perederii M.A., Utilization of petroleum residues under microwave irradiation, Chemical Engineering Journal 292 (2016) 315–320
Tsodikov M.V., Ellert O.G., Nikolaev S.A., Arapova O.V., Konstantinov G.I., Bukhtenko O.V., Vasil'kov A.Yu., 2017, The role of nanosized nickel particles in microwave-assisted dry reforming of lignin, Chem. Eng. J., 309, 628–637.
Yamada Y., Yoshida H., Kouno K., Kobayashi Y., 2010, Iron carbide films produced by laser deposition, J. Phys.: Conf. Series, 217, 01209.
Yao Y., Falk L.K.L., Morjan R.E., Nerushev, O.A. Campbell E.E.B., 2004, Synthesis of carbon nanotube films by thermal CVD in the presence of supported catalyst particles. Part II: the nanotube film, J. Mater. Sci. - Mater. Electron., 15, 583-594.
Yunpu W., Leilei D., Liangliang F., Shaoqi S., Yuhuan L., Roger R., 2016, Review of microwave-assisted lignin conversion for renewable fuelsand chemicals, J. Anal. Appl. Pyrolysis, 119, 104–113.
Zhang X.L., Lee C.S-M., Mingos D.M.P., Hayward D.O., 2003, Carbon dioxide reforming of methane with Pt catalysts using microwave dielectric heating, Catal. Lett., 88 (3–4), 129–139.